



Planar Reconfigurable Plasma Leaky-Wave Antenna with Electronic Beam-Scanning for MIMO Applications

Hend A. Malhat¹ · Abdelkarim S. Elhenawy² · Saber H. Zainud-Deen¹ · Noha A. Al-Shalaby²

Accepted: 28 August 2022 / Published online: 14 September 2022
© The Author(s) 2022

Abstract

A planar leaky-wave antenna (LWA) based on the reconfigurable conductivity of the plasma is designed for MIMO applications with electronic beam scanning capability. 112-semi-elliptical ionized plasma gratings are encased by plexiglass grating filled with a noble gas. These gratings are printed on a metal-backed dielectric substrate with total dimensions of $L \times W_s \times h = 241 \times 262.5 \times 2.67 \text{ mm}^3$. A coplanar fed printed Yagi-Uda like dipole antenna is integrated with the LWA to launch the required excitation waves. The radiated beam direction, gain, and the side lobe level are adjusted by controlling the periodicity of ionized/non-ionized plasma gratings. The antenna is compact in construction and has a high gain. A fan-shaped beam is obtained from the LWA semi-elliptical arrays with different aspect ratios. The effect of ON/OFF plasma periodicity configurations on the radiation characteristics at fixed frequency is investigated. At 10.1 GHz, the beam is electronically scanned from -28 to 34° using different periodicities with high gain of 20 dB and radiation efficiency of 74%. The mutual coupling between two LWA elements is investigated and is reduced to -35 dB. Four LWA elements are arranged in MIMO structure for a high data rate application. The envelope correlation coefficient of 0.0002 and diversity gain of 9.9998 dB are achieved.

Keywords MIMO · Plasma · Leaky-wave antenna · Reconfigurable

1 Introduction

Multiple-Input Multiple-Output (MIMO) technology is based on simultaneous transmission and reception of data signals to improve the channel capacity and data rates. MIMO systems employ multiple antenna elements at the transmitter and receiver [1]. MIMO systems are suitable for 5G communication systems due to their advantages such as high data rates, high spectral efficiency, immunity to multipath fading and good reliability. Antennas employed in MIMO systems are characterized by compact size, low cost and beam

✉ Hend A. Malhat
er_honida1@yahoo.com

¹ Faculty of Electronic Engineering, Menoufia University, Menouf, Egypt

² Faculty of Engineering, Kafrelsheikh University, Kafr El-Shaikh, Egypt

scanning capability [2]. In comparison with other solutions offering MIMO solutions [3, 4], reconfigurable LWA elements provide electronically controllable backfire-to-end-fire full-space scanning, in addition to beam shaping [5]. However, the mutual coupling is increased when numerous antennas are utilized in array structures, which degrades the array performance [6, 7]. When the elements isolation level is decayed, high impedance mismatching, low efficiency, and deflection of the radiation pattern occurs. Suppressing the interaction between multi-antenna systems were introduced via many solutions such as metamaterial, photonic bandgap and 180° hybrid coupler [8, 9].

Different mechanical and electrical beam-scanning techniques are introduced in the literature. The mechanical scanning is achieved using electric motors and MEMS devices to rotate the antenna structure. Mechanical scanning technique becomes difficult and undesirable for large-size antennas [10, 11]. The solutions for the mechanical problems are achieved using electronic switches such as PIN diodes, varactor diodes, or FET transistors. The electronic scanning techniques are expensive and loss at millimeter-wave frequencies [12]. Optical switching techniques use photoconductive switches in antenna structures can be considered. Recently, beam scanning techniques based on materials with reconfigurable properties such as graphene, liquid crystal, ferrite, and plasmonics are employed by controlling their permittivity or conductivity [13, 14]. High-gain beam-scanning techniques are used in long-distance wireless communication applications such as airborne platforms, radar and satellite communications. The conventional types of high-gain antennas are reflectors, lenses, reflectarrays, transmitarrays, and direct-radiating phased arrays [15–18].

Leaky-wave antennas (LWAs) radiate high directive beams in different directions at the operating frequency. Their leakage lengths, control the beamwidth. of the LWAs, are characterized by planar, simple and low-profile structures with integrated excitation. Conventional LWAs have the property of sweeping the main beam direction with frequency. It has limited applications in modern communication systems such as point-to-point communications which require beam sweeping at the same frequency [19]. LWA structures are studied using different geometries such as one dimensional (1D) and two dimensional (2D) structures. Periodic structures are introduced in [20, 21]. The leakage from 2D-LWAs propagates radially outward from the planar interface with beam-width scanning from pencil beam at broadside to conical beam at other angles with frequency sweeping [22].

Two techniques are employed in LWAs designs. The first technique uses partially reflecting surface such as 2D periodic slots, patches, strips, wires and multiple-dielectric layers. The second technique uses multiple 1D LWAs [23–26]. In [27], the main beam scanning capability is achieved at a single frequency for 1D LWAs using reconfigurable graphene material in the THz range. In [28], continuous metal semi-circular strips 2D LWA is designed with pencil and sector-conical beam patterns scanning around 21.2 GHz. Recently, ionized inert gases (plasma) encased by dielectric tubes are used in reconfigurable antenna applications [29, 30]. Plasma material's conductivity can be controlled by using a DC voltage source, RF fields, or magnetic coupling loop. Different plasma-based antennas such as dipole, curl, reflectarray, lens and magneto-electric dipole are investigated in [31, 32]. Plasma-based antennas provide a high reconfigurable structure due to the ability to control the of their electrical properties.

In this paper, planar plasma leaky-wave antenna with beam scanning capability at fixed frequency is proposed. The radiated beam shape is varied from pencil beam at broadside to sector-conical beam at the other angles. A parametric study of plasma electrical conductivity and ionized gas dimensions on the LWA radiation characteristics is introduced. An array of two elements with a perforated substrate is proposed for reconfigurable dual beams at a fixed frequency. Finally, an array of four elements is designed for MIMO system

applications. The MIMO design characteristics are studied and calculated as envelope correlation coefficient and diversity gain. The results are investigated using the finite integral technique (FIT) [32].

2 Design of Semi-Elliptical Gratings LWA

The structure of the single element of the reconfigurable semi-elliptical gratings plasma LWA is shown in Fig. 1. The LWA element consists of 112- semi-elliptical plasma gratings encased by plexiglass gratings. They are mounted on a grounded RT/duroid 6010 LM substrate with $\epsilon_{rs} = 10.2$. Each grating is 0.2 mm thick plexiglass tube with $\epsilon_{rp} = 3.4$, width w and filled with argon gas of height h_p . It has a cross-section of semi-elliptical structure with semi major-axis, b , semi minor-axis, a , and aspect ratio, $c = b/a$. Each point locus on the semi-elliptical grating is calculated from:

$$\frac{y^2}{b^2} + \frac{x^2}{a^2} = 1 \tag{1}$$

$$b(m) = b_0 + \frac{P}{7}(m - 1) \tag{2}$$

where m is the grating number, $b_0 = 21\text{mm}$ is the first grating semi-major radius, and P is LWA periodicity. According to [33], when $c = 1$ circular grating LWA is produced to radiates pencil beam gain which results in circular gratings. The total dimensions of the LWA are $L \times W_s \times h = 241 \times 262.5 \times 2.67\text{mm}^3$. The semi-elliptical gratings are filled with a low-pressure noble gas (argon), its relative dielectric constant is represented by the Drude model and is described by [33]:

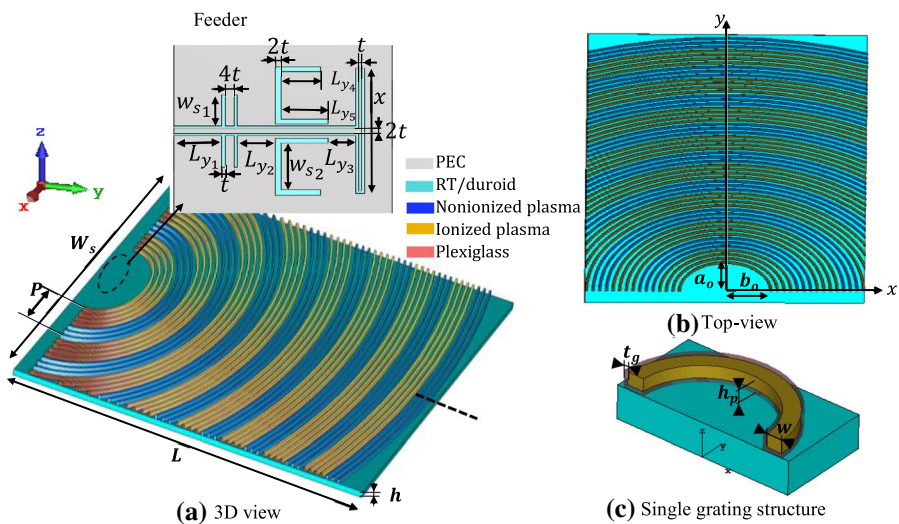


Fig. 1 3D plasma leaky wave antenna. a 3D configuration, b Top view, c Single grating structure

$$\epsilon_r = \epsilon_o \left[1 - \frac{\omega_p^2}{\omega(\omega - j\nu_p)} \right] \tag{3}$$

$$\omega_p = \sqrt{\frac{n_e e^2}{m_e \epsilon_o}} \tag{4}$$

where ω, ω_p and ν_p are the angular operating, plasma, and collision frequencies respectively. n_e is the ionized electron density, e and m_e are the electron charge and mass. The plasma medium is considered as a dielectric material for non-ionized plasma (OFF-state for $\omega > \omega_p$). The plasma medium is considered as a conducting material for the ionized plasma (ON-state for $\omega < \omega_p$). According to the required radiated beam direction, each plasma grating is biased between the ON- and OFF-states with $\nu_p = 2\text{GHz}$. The applied voltage V can be calculated using [33].

$$V = \left(\frac{n_e \sqrt{ekT_e} h_p^2}{\epsilon_0} \right)^{2/3} \tag{5}$$

where T_e is the electron temperature and h_p is the plasma height. 2D LWA excitation requires cylindrical wave source, which is obtained using a grounded Yagi-Uda like antenna feeder introduced in [34]. The feeder consists of a dipole antenna with width $x = 4.58$ mm, and the reflector dimensions of $t = 0.105$ mm, $w_{s2} = 2.45$ mm, $L_{y3} = 0.92$ mm, $L_{y4} = 1.33$ mm, and $L_{y5} = 1.56$ mm to reduce the power loss in the back-lobe direction. Two matching stubs with $w_{s1} = 1.365$ mm, $L_{y1} = 2.52$ mm and $L_{y2} = 1.26$ mm are added to the structure as shown in Fig. 1. The plasma LWA with 112 gratings is divided into periods with a length of 12.86 mm which contains 7 plasma gratings. Each period has four ON-states gratings with ionized plasma and three OFF-states gratings with non-ionized plasma which is represented by the code 1,111,000. Figure 2 shows the effect of plasma frequency ω_p on the material dielectric constant. It can be noted that the real part ϵ' is decreased with increasing ω_p while the imaginary part ϵ'' is increased, hence the conductivity of the material is increased with increasing ω_p .

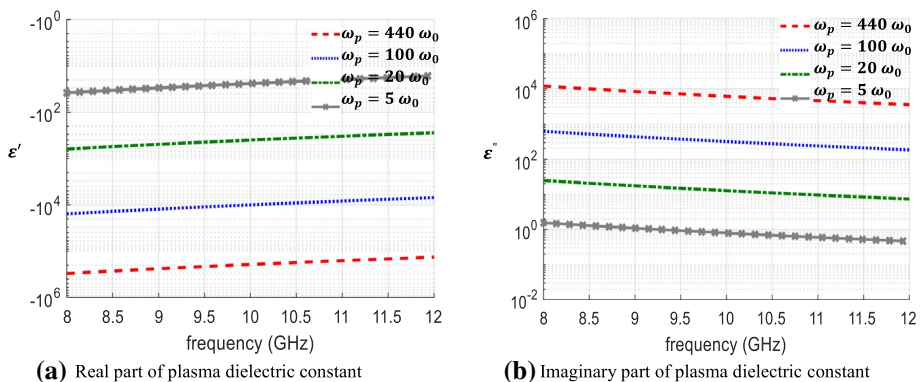


Fig. 2 Effect of plasma frequency ω_p on material dielectric constant

3 Parametric Study

3.1 Effect of Plasma Frequency ω_p

When the plasma frequency ω_p is increased, the ON-state plasma grating conductivity is increased. The applied ionization voltage excites free electrons with high density to convert the plasma gratings from dielectric state to conducting state. Figure 3 shows the effect of varying ω_p from 50GHz to 4.4THz for the 1,111,000 Code-LWA arrangement. The impedance matching bandwidth (BW) is unaffected by the plasma ionization values due to the feeder position away from the LWA effective area. The plasma gratings are responsible for directing the beam. The peak gain is increased with increasing ω_p , and the beam disappears when the plasma gratings are non-ionized.

3.2 Plasma Gratings Dimensions

The semi-circular gratings LWA with aspect ratio $c = 1$ results in a high gain pencil beam which is preferred in satellite communications and radar systems. The dimensions of the LWA are studied to get the optimum values as shown in Table 1. The effect of changing the plasma grating height, h_p , on S_{11} of the LWA with code 1,111,000 is shown in Fig. 4a. When the plasma height h_p is increased, more gas is included in the grating, which increases the free electron density. The impedance matching BWs are 1.41 GHz, 1.52 GHz, 1.33 GHz, and 1.27 GHz for h_p equal 1.5 mm, 1.0 mm, 0.75 mm, and 0.5 mm, respectively. Figure 4b shows the gain patterns variation versus angle at 10.1 GHz for different values of h_p . The peak gain is increased by increasing h_p with a little shift in the main beam direction due to the effect of grating edges. Peak gains of 23 dBi, 23 dBi, 22.4 dBi and 21.7 dBi are obtained for h_p equal 1.5 mm, 1.0 mm, 0.75 mm, and 0.5 mm, respectively. The main beam direction angle/SLL are $4^\circ/-11.5$ dB, $1^\circ/-14.4$ dB, $0^\circ/-14$ dB and $-2^\circ/-12.6$ dB, respectively.

Figure 5 shows the effect of changing plasma grating width w at $h_p = 1$ mm on S_{11} and gain pattern of the LWA. Increasing the plasma grating width, w improves the matching BW up to 15.09% for $w = 1.36$ mm compared with 4.65% for $w = 0.5$ mm. The peak gain is increased to 23 dBi at a deflection angle of 7 degrees for $w = 1.36$ mm compared with

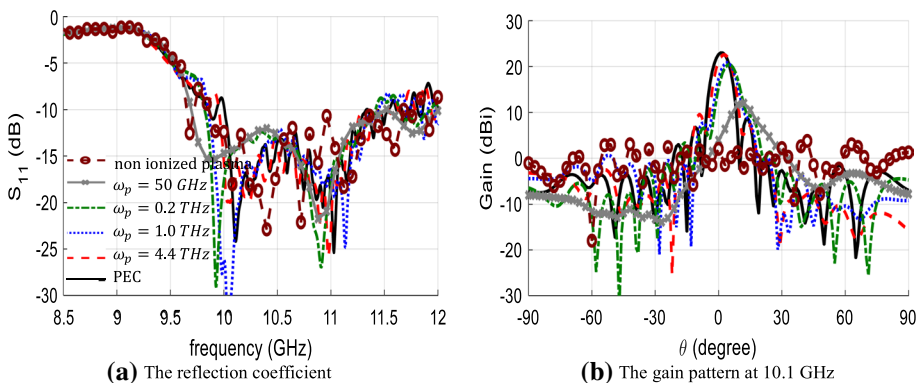


Fig. 3 The effect plasma frequency ω_p on 1,111,000 LWA with $c = 1$, $P = 7$, of $h_p = 1$ mm, $w = 1.26$ mm and $\nu_p = 2$ GHz

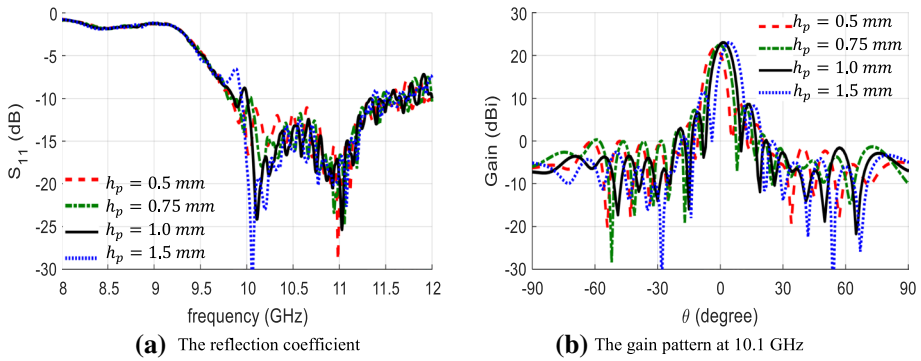


Fig. 4 The effect of h_p plasma height on semi-circular 1,111,000 LWA with $c=1$, $P=7$, $w=1.26$ mm, $\omega_p=4.4$ THz and $\nu_p=2$ GHz

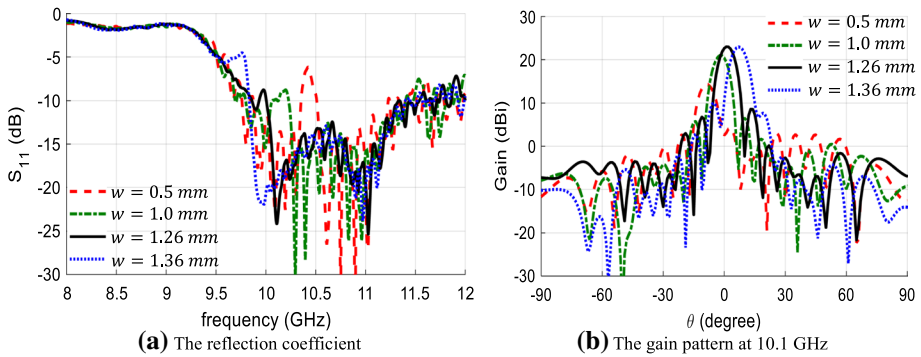


Fig. 5 The effect of w grating width on semi-circular 1,111,000 LWA with $c=1$, $P=7$, of $h_p=1$ mm, $\omega_p=4.4$ THz and $\nu_p=2$ GHz

14.3 dBi gain and a deflection angle of -9° for $w=0.5$ mm from the broadside direction. An improvement in the SLL is noticed from -12.9 to -14.4 dB for $w=1.36$ mm and $w=1.26$ mm, respectively. The optimum grating width is $w=1.26$ mm which produces $BW=14.1\%$ (from 10.02 to 11.54 GHz), peak gain of 23 dBi, SLL of -14.4 dB and beam deflection angle of 1° . Figure 6 shows the frequency-scanning at different frequencies of LWAs. Figure 7 shows the frequency response of gain and efficiency of the LWA. The peak gain is 22 dBi which is nearly constant in the frequency band from 0.02 to 10.5 GHz with variation of ± 1 dBi. High efficiency of 74.3% is obtained at 10.1 GHz.

4 Reconfigurable Semi-Circular Gratings Plasma LWA

The optimized dimensions of the semi-circular gratings LWA are $h_p=1$ mm and $w=1.26$ mm. The reconfigurable conductivity of ionized plasma is used to achieve electronic beam scanning without affecting the LWA physical structure. By ionizing/non-ionizing the plasma enclosed in the gratings with different periodicity, P , the beam is directed to different angles at fixed frequency. The 112- plasma gratings are divided into periods each have (m, n) of (ON, OFF) pair of plasma gratings. The first number represents the number

Fig. 6 LWA operation on semi-circular 1,111,000 LWA with $c = 1$, $P = 7$, $h_p = 1.0$ mm, $w = 1.26$ mm, $\omega_p = \infty$, and $\nu_p = 2$ GHz

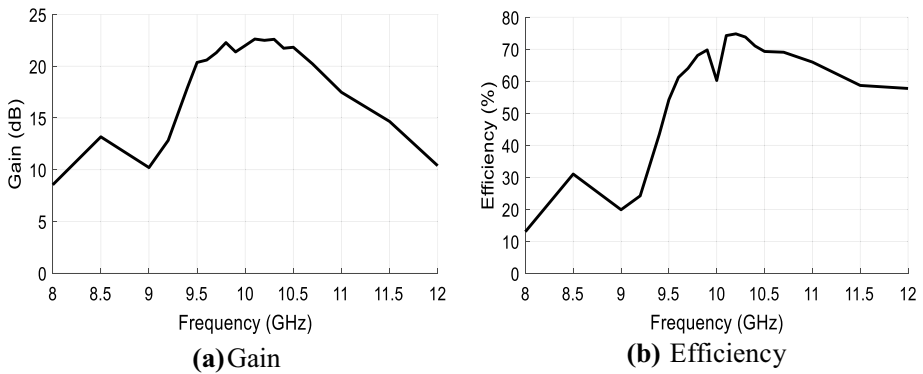
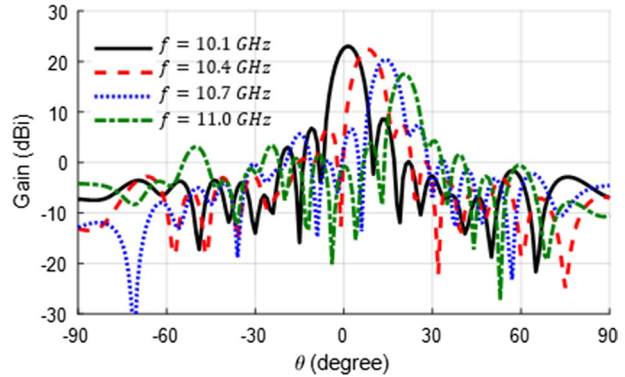


Fig. 7 The characteristics of semi-circular 1,111,000 plasma gratings LWA with $c = 1$, $P = 7$, of $h_p = 1$ mm, $\omega_p = 4.4$ THz and $\nu_p = 2$ GHz, and $w = 1.26$ mm

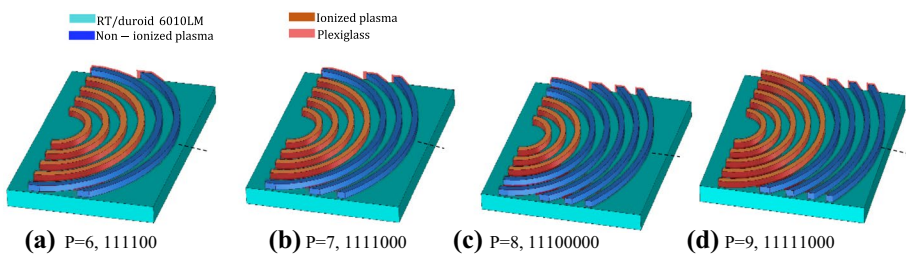


Fig. 8 Configuration of reconfigurable plasma gratings LWA with different periodicity

of ionized plasma gratings, and the second number represents the non-ionized plasma gratings. Figure 8 shows the configuration of different periods P of the LWA coded by (ON, OFF) plasma states. Four periods with 6, 7, 8, and 9 are investigated. For example, when $P = 6$ gratings coded by 111,100 has the first four plasma gratings ON and the following two plasma gratings OFF. Each code is responsible for directing the beam toward a specific direction at the same operating frequency $f_0 = 10.1$ GHz.

For $P=6$, different codes are studied (5, 1), (4, 2), (3, 3), and (2, 4). At 10.1 GHz the beam is scanned from -28 to -14° with peak gain of 18.5 ± 0.6 dBi. For $P=7$, the codes (5, 2), (4, 3), (3, 4), and (2, 5) are investigated. The beam is scanned from -11 to 9° with peak gain of 20.4 ± 2.6 dBi at 10.1 GHz. For $P=8$, the studied codes are (6, 2), (5, 3), (4, 4), (3, 5) and (2, 6) show scanning beams from 8 to 23° . For $P=9$, the studied codes are (6, 3), and (5, 4). The beam is scanned from 30 to 34° with high gain. As noticed, an overall beam scanning range of -28° to 34° at fixed frequency 10.1 GHz is achieved. The SLL of the beams varies between -15.5 and -8.2 dB. Table 2 introduces a comparison between different grating-codded plasma LWA with different periodicity, P . The 3D beam patterns at the codes that radiate the maximum gains are shown in Fig. 9. The peak gains are 17.5 dBi for $P=9$ code (5, 4), 20.3 dBi for $P=8$ code (3, 5), 23 dBi for $P=7$ code (4, 3), and 19.3 dBi for $P=6$ code (4, 2). The effect of using 2D LWA configuration is clear in the scanning BW from pencil beam to sector-conical beam.

Table 3 shows a comparison between the proposed plasma gratings LWA with 2D LWA introduced in the literature. It shows that the proposed compact structure provides the widest scanning angle range with acceptable efficiency and gain.

5 Two Elements Antenna Array

An array composed of two plasma gratings LWA is designed to provide two modes of operation. The first mode uses the array structure as a switched antenna, where each element is used separately to provide single beam scanning in different angles with different

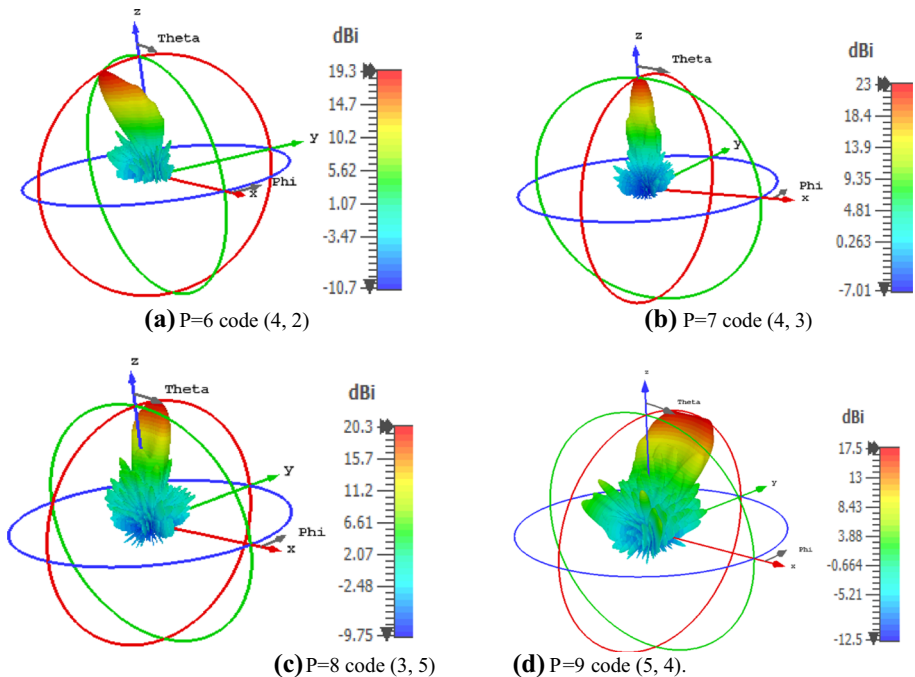


Fig. 9 3D gain patterns for highest gain code configurations at 10.1 GHz

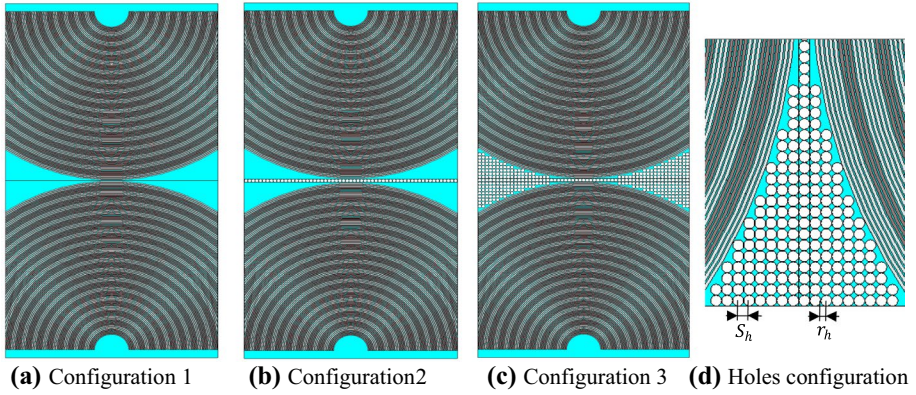
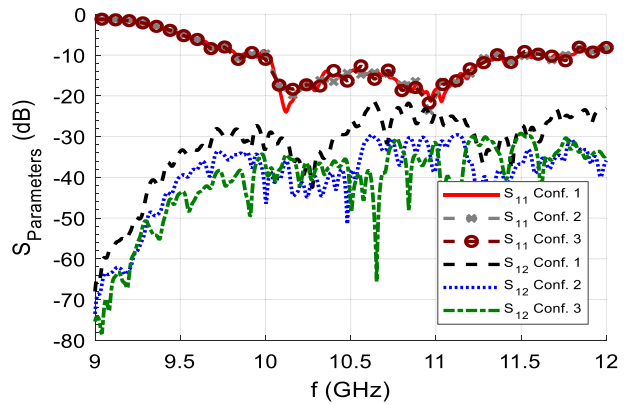


Fig. 10 Different configurations used to minimize S_{12}

Fig. 11 Comparison between S_{12} for different configurations



beamwidths. The second mode uses both antenna elements together to provide a dual-beam scanning. Figure 10 presents different configurations of the two-element array to minimize the mutual coupling effect between the two antenna elements. The perforated structure is employed to hold the array elements in a single substrate. The connected regions are perforated to match the substrate dielectric constant to air. The optimum configuration uses a perforated substrate between the two elements with effective permittivity given by [35],

$$\epsilon_{r_{eff}} = \epsilon_r(1 - \alpha) + \alpha \tag{6}$$

$$\alpha = \frac{\pi r_h^2}{\sqrt{3}/2 * s_h^2} \tag{7}$$

where r_h is the radius of the air holes, and s_h is the separation between the holes centres. Minimum $\epsilon_{r_{eff}} \simeq 1.86$ is used. Figure 11 indicates the effect of the different configurations on the mutual coupling between both antennas. Configuration 3 employs a perforated substrate which minimizes the coupling to about -30 dB. The 3D radiated beams at 10.1 GHz

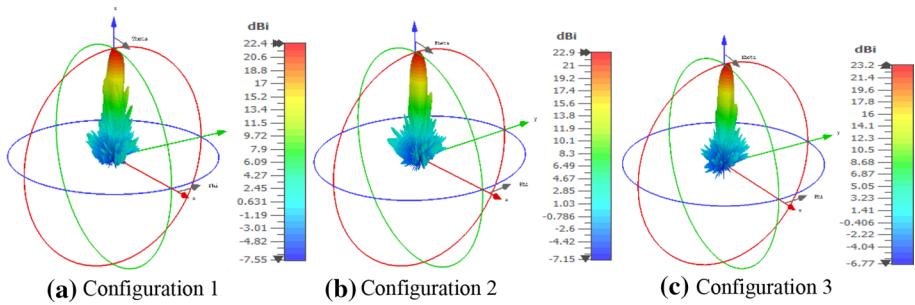


Fig. 12 3D gain patterns different configurations at 10.1 GHz for [P1=7 code (4, 3), P2=7 code (4, 3)]

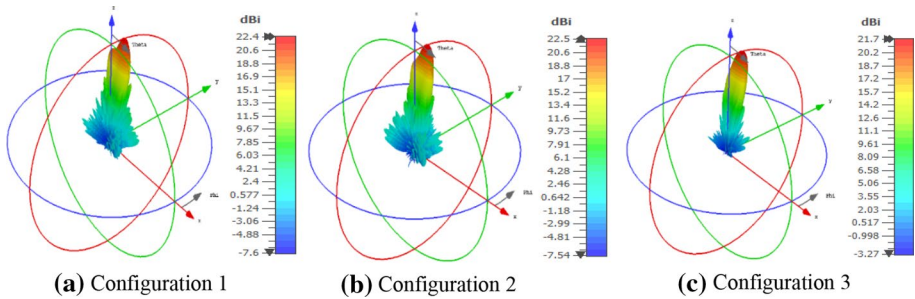


Fig. 13 3D gain patterns different configurations at 10.5 GHz for [P1=7 code (4, 3), P2=7 code (4, 3)]

and 10.5 GHz respectively for the different configurations are shown in Fig. 12, and Fig. 13. Configuration 3 introduces a directive beam with low side-beam characteristics which is desired for beam scanning applications. The simulation of two modes of operation is achieved using configuration 3 as shown in Fig. 14. A single reconfigurable beam is obtained for each port with different codes and dual reconfigurable beams are achieved using a combination of these single beams at 10.1 GHz.

6 Four Elements Antennas Array for MIMO Systems

MIMO antennas are desired in communication systems that require fast data rates, improved capacity and link reliability. Figure 15 shows a MIMO system composed of 4 antenna elements with 90° orientation angle. The length of each antenna element is reduced to 42 plasma gratings for simplicity. The same concept can be applied for larger gratings numbers, with a perforated substrate between each of them of length λ_g . The coupling between the first element and MIMO elements is shown in Fig. 16. The coupling is minimized between the elements of the MIMO system below the level of -30 dB. The radiated beams of each element at 10.1 GHz and 10.5 GHz are shown in Figs. 17 and 18. The envelope correlation coefficient, ECC, and diversity gain, DG, are simulated to determine the independency of MIMO elements on each other and the effect of the diversity scheme on the radiated power is shown in Fig. 19. The ECC is determined from the antenna isolation, S_{21} without measuring the antennas' radiation

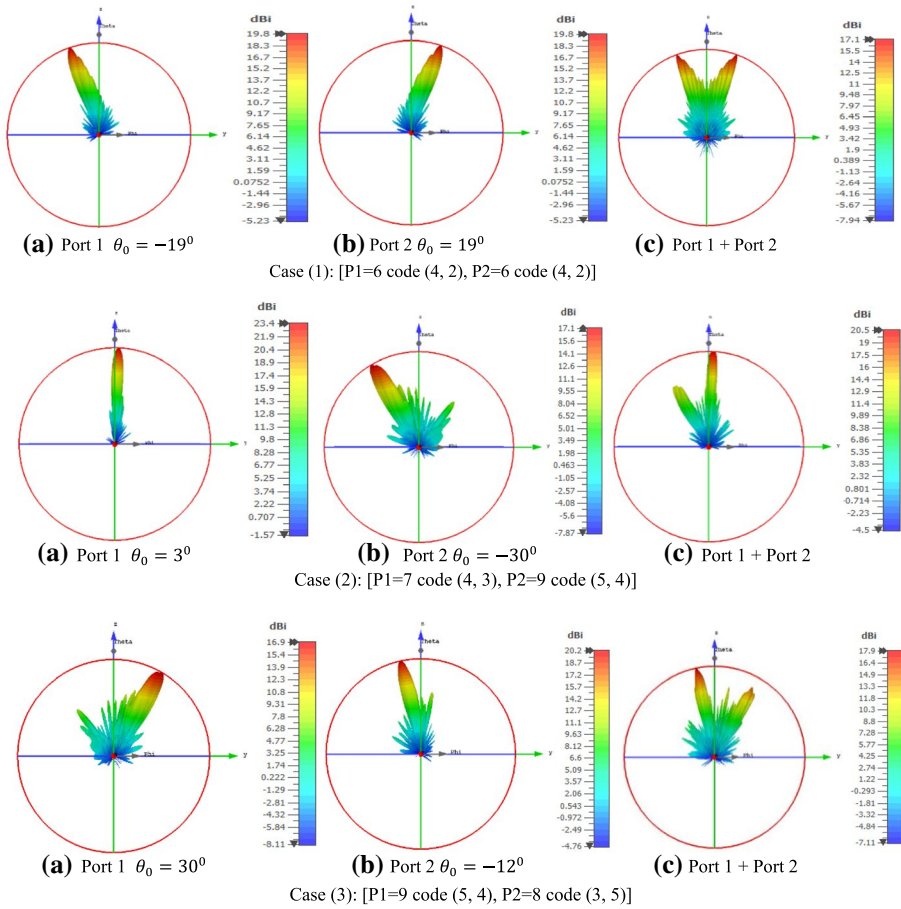


Fig. 14 3D gain patterns at 10.1 GHz for different Codes

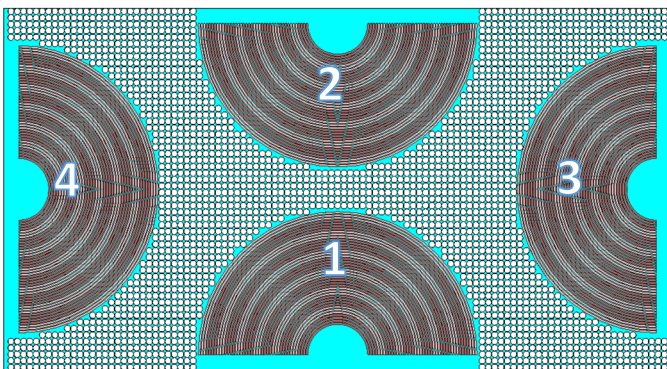


Fig. 15 Proposed Configuration

Fig. 16 The coupling between the first element and MIMO elements

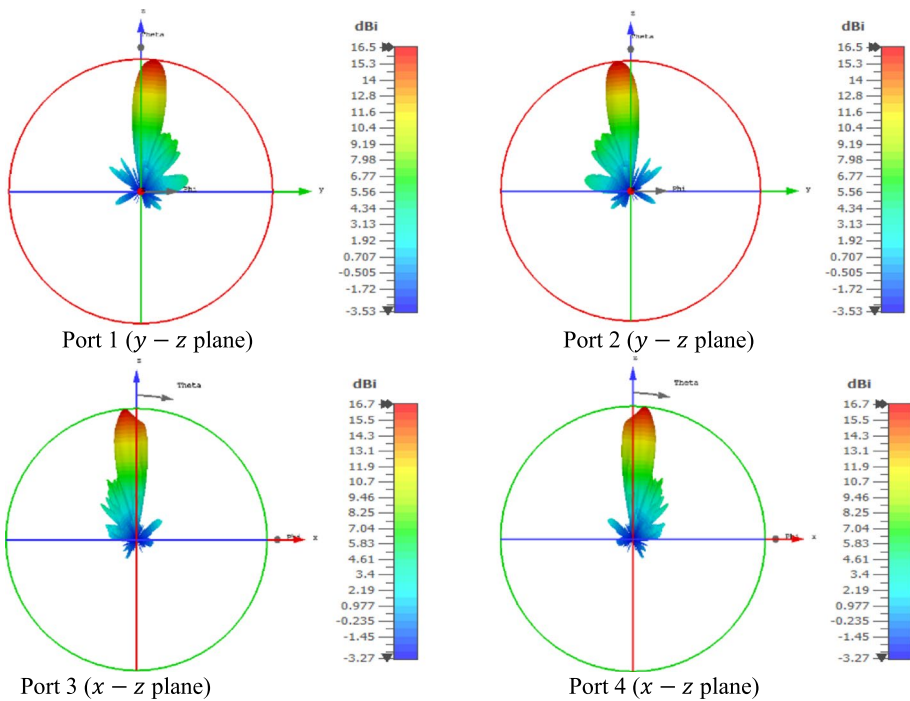
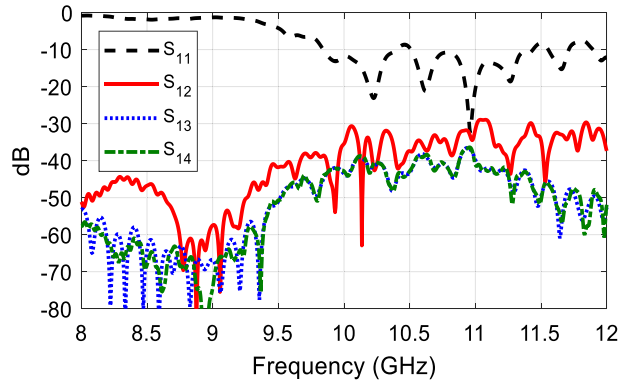


Fig. 17 3D gain patterns at 10.1 GHz for Code $P_1 = P_2 = P_3 = P_4 = 7$ (4, 3)

patterns. Because, the antennas produce highly correlated radiation pattern, then they will also have low isolation for antenna reciprocity. The receiving element receive the transmitted radiation pattern energy proportional to how correlated the antennas' radiation patterns. ECC and DG are calculated from:

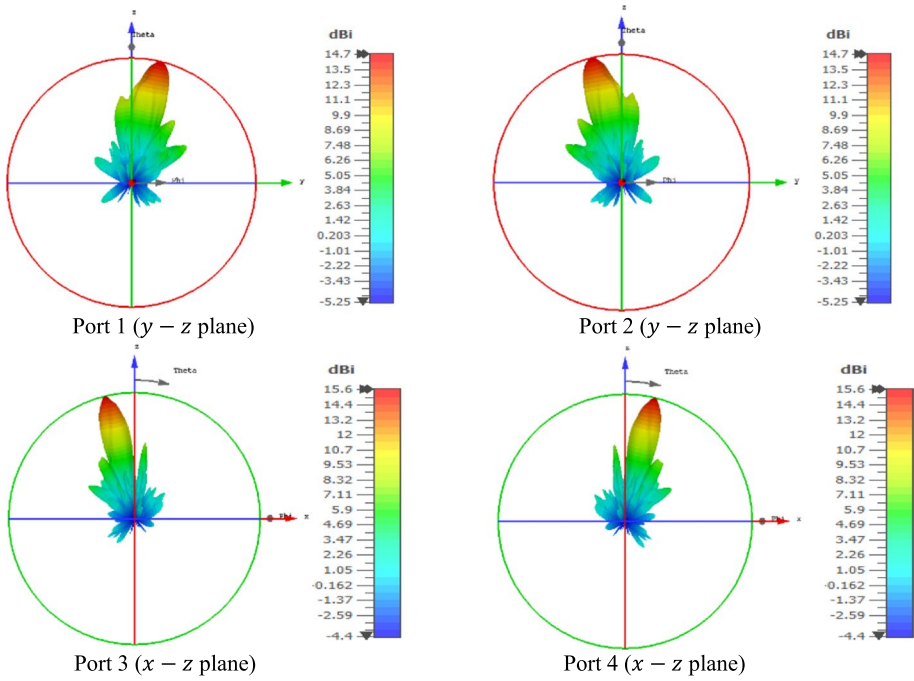


Fig. 18 3D gain patterns at 10.5 GHz for Code P1 = P2 = P3 = P4 = 7 (4, 3)

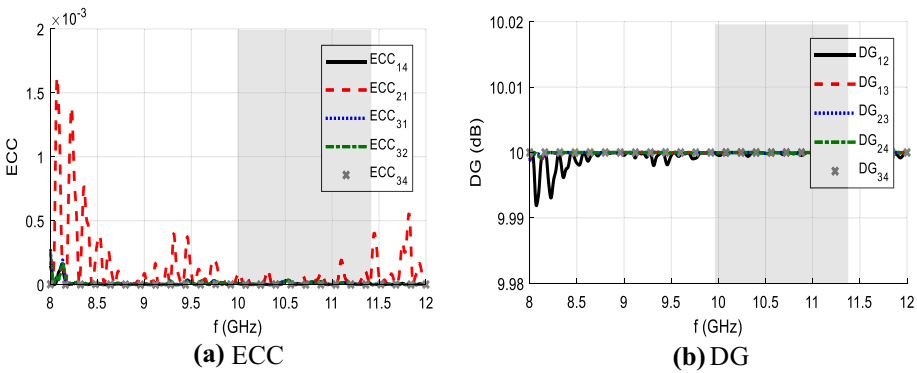


Fig. 19 MIMO antenna parameters

$$ECC = \rho_{e_{ij}} = \frac{|S_{ii}^* * S_{ij} + S_{ji} * S_{jj}|^2}{(1 - |S_{ii}|^2 - |S_{ij}|^2)(1 - |S_{ji}|^2 - |S_{jj}|^2)} \tag{8}$$

$$DG = 10\sqrt{1 - |\rho_{e_{ij}}|^2} \tag{9}$$

Table 1 The optimum dimensions of the plasma gratings LWA

Substrate			
ϵ_r	h	W_s	L
10.2	2.67mm	262.5mm	241mm
Grating			
t_g	h_p		w
0.2mm	1mm		1.26mm

Table 2 Comparison between radiation characteristics using different codes of plasma gratings LWA at 10.1 GHz

Period	Code	Main beam	Gain	SLL
6	2, 4	-28	17.7	-10.3
6	3, 3	-24	19.2	-9.5
6	4, 2	-19	19.3	-8.8
6	5, 1	-14	18.3	-9.9
7	1, 6	-11	17.8	-10.5
7	2, 5	-6	22	-13.3
7	3, 4	-3	22.4	-14.9
7	4, 3	1	23	-14.4
7	5, 2	4	22.7	-15.5
7	6, 1	9	19.4	-11.8
8	2, 6	8	19.3	-10.4
8	3, 5	12	20.3	-10.8
8	4, 4	16	19.9	-11.4
8	5, 3	19	19.2	-11.8
8	6, 2	23	17.2	-10.6
9	5, 4	30	17.2	-8.2
9	6, 3	34	15.5	-8.7

Table 3 Comparison between the proposed plasma gratings LWA with 2D LWA introduced in the literature

Ref	Operating frequency (GHz)	Scanning ability	Efficiency (%)	Area ($\lambda_o \times \lambda_o$)	Gain (dBi)
[36]	19.48	17°	57.6	6.6×6.6	18.55
[37]	18	N/A	96	2π(16.8×16.8)	N/A
[38]	237.5	50°	56	35.6×6.7	28.5
[39]	42	54°	89	18.6×13	29.2
[40]	32	28°	89.4	30	20.43
This work	10.1	62°	74	8×8.7	23

The *ECC* values obtained from Eq. (8) are very low ~ 0.0002 within the operating frequency, which is considered to be excellent diversity performance with uncorrelated far-field patterns of the MIMO antennas. The diversity gain for all the antenna elements is more than 9.9998 dB which is very close to the ideal value of 10 dB.

7 Conclusion

This paper introduces an investigation of reconfigurable planar LWA using controlled conductivity of the plasma material for beam steering applications. The effect of plasma conductivity is investigated at different plasma frequencies. The plasma LWA with 1,111,000 code introduces radiation with BW of 1.52 GHz, a gain of 23 dBi, and SLL of -14.4 dB with pencil beam at 1° shifted from the broadside direction. The beam is scanned at a single frequency of 10.1 GHz by controlling the conductivity of plasma gratings from -28° degrees up to 34° degrees with a maximum gain of 23 dBi. A comparison between the radiation characteristics of plasma gratings LWA for different codes arrangements is explained. The antenna is employed in the MIMO system with four elements. The ECC values are very low ~ 0.0002 and the diversity gain is 9.9998 dB.

Author Contributions All the authors contribute equally in this paper.

Funding Open access funding provided by The Science, Technology & Innovation Funding Authority (STDF) in cooperation with The Egyptian Knowledge Bank (EKB). There is No funds, grants, or other support was received to conduit this study.

Data Availability The program is available upon request.

Declarations

Conflict of interest The authors have no conflicts of interest or competing interests to declare that are relevant to the content of this article.

Ethical Approval There is no ethical approval is required.

Informed consent Informed consent was obtained from all individual participants included in the study.

Open Access This article is licensed under a Creative Commons Attribution 4.0 International License, which permits use, sharing, adaptation, distribution and reproduction in any medium or format, as long as you give appropriate credit to the original author(s) and the source, provide a link to the Creative Commons licence, and indicate if changes were made. The images or other third party material in this article are included in the article's Creative Commons licence, unless indicated otherwise in a credit line to the material. If material is not included in the article's Creative Commons licence and your intended use is not permitted by statutory regulation or exceeds the permitted use, you will need to obtain permission directly from the copyright holder. To view a copy of this licence, visit <http://creativecommons.org/licenses/by/4.0/>.

References

1. Alibakhshikenari, M., Virdee, B. S., Azpilicueta, L., Naser-Moghadasi, M., Akinsolu, M. O., See, C. H., Liu, B., Abd-Alhameed, R. A., Falcone, F., Huynen, I., & Denidni, T. A. (2020). A comprehensive survey of metamaterial transmission-line based antennas: Design, challenges, and applications. *IEEE Access*, 8, 144778–144808.
2. Yang, B., Yu, Z., Dong, Y., Zhou, J., & Hong, W. (2017). Compact tapered slot antenna array for 5G millimeter-wave massive MIMO systems. *IEEE Transactions on Antennas and Propagation*, 65(12), 6721–6727.
3. Petit, L., Dussopt, L., & Laheurte, J. (2006). MEMS-switched parasitic-antenna array for radiation pattern diversity. *IEEE Transactions on Antennas and Propagation*, 54(9), 2624–2631.

4. Forenza, A., & Heath, R. W. (2006). Benefit of pattern diversity via two-element array of circular patch antennas in indoor clustered MIMO channels. *IEEE Transactions on Communications*, *54*(5), 943–954.
5. Javanbakht, N., Syrett, B., Amaya, R. E., & Shaker, J. (2021). A review of reconfigurable leaky-wave antennas. *IEEE Access*, *9*, 94224–94238.
6. Althuwayb, A. A. (2021). Low-interacted multiple antenna systems based on metasurface-inspired isolation approach for MIMO applications. *Arabian Journal for Science and Engineering*, 1–10.
7. Alibakhshikenari, M., Virdee, B. S., Parchin, N. O., Shukla, P., Quazzane, K., See, C. H., Abd-Alhameed, R., Falcone, F., & Limiti, E. (2020). Isolation enhancement of densely packed array antennas with periodic MTM-photonic bandgap for SAR and MIMO Systems. *IET Microwaves, Antennas & Propagation*, *14*(3), 183–188.
8. Maleki, A., Oskoue, H. D., & Mohammadi Shirkolaei, M. (2021). Miniaturized microstrip patch antenna with high inter-port isolation for full duplex communication system. *International Journal of RF and Microwave Computer-Aided Engineering*, *31*(9), e22760.
9. Alibakhshikenari, M., Virdee, B. S., See, C. H., Abd-Alhameed, R., Hussein Ali, A., Falcone, F., & Limiti, E. (2018). Study on isolation improvement between closely-packed patch antenna arrays based on fractal metamaterial electromagnetic bandgap structures. *IET Microwaves, Antennas and Propagation*, *12*(14), 2241–2247.
10. Liu, L., Wang, J., Yin, X., & Chen, Z. N. (2018). Wide-angle beam scanning leaky-wave antenna using spoof surface plasmon polaritons structure. *Electronics*, *7*, 348.
11. Sarkar, A., & Lim, S. (2022). Annular surface plasmon polariton-based frequency-scanning leaky-wave antenna for full azimuth coverage. *IEEE Transactions on Antennas and Propagation*, *70*(1), 180–188.
12. Uchendu, I., & Kelly, J. (2016). Survey of beam steering techniques available for millimeter wave applications. *Progress In Electromagnetics Research B*, *68*, 35–54.
13. Bernhard, J. T. (2007). *Reconfigurable antennas*. Morgan and Claypool.
14. Zainud-Deen, S. H., Mabrouk, A. M., Malhat, H. A. (2017) Frequency tunable graphene metamaterial reflectarray. In *2017 XXXIInd general assembly and scientific symposium of the international union of radio science (URSI GASS), Montreal, QC* (pp 1–4).
15. Yang, Y., Yuan, C., & Qian, B. (2014). A beam steering antenna for X-band high power applications. *AEU - International Journal of Electronics and Communications*, *68*(8), 763–766.
16. Zainud-Deen, S. H., Malhat, H. A., & Elshalaby, N. A. (2019). Broadband transmitarray for satellite applications in Ku band. *Wireless Personal Communications*, *107*(1), 149–158.
17. Malhat, H., Zainud-Deen, S., Hassan, W., & Awadalla, K. (2015). Radiation characteristics enhancement of dielectric resonator antenna using solid/discrete dielectric lenses. *Advanced Electromagnetics*, *4*(1), 1–9.
18. Nayeri, P., Yang, F., & Elsherbeni, A. Z. (2015). Beam-scanning reflectarray antennas: A technical overview and state of the art. *IEEE Antennas and Propagation magazine*, *57*(4), 32–47.
19. Oliner, A. A., & Jackson, D. R. (2007). Leaky-wave antennas. In J. L. Volakis (Ed.), *Antenna engineering handbook (4th edn)*. McGraw-Hill.
20. Jackson, D. R., Caloz, C., & Itoh, T. (2012). Leaky-wave antennas. *Proceedings of the IEEE*, *100*(7), 2194–2206.
21. Kallel, A., Sokoloff, J., & Callegari, T. (2014). Leaky-wave plasma antenna with tunable radiation angle. *Microwave and Optical Technology Letters*, *56*(11), 2601–2604.
22. Sengupta, S., Jackson, D. R., Almutawa, A. T., Kazemi, H., Capolino, F., & Long, S. A. (2020). A Cross-shaped 2-d periodic leaky-wave antenna. *IEEE Transactions on Antennas and Propagation*, *68*(3), 1289–1301.
23. Sengupta, S., Jackson, D. R., Almutawa, A. T., Kazemi, H., Capolino, F., & Long, S. A. (2019). Radiation properties of a 2-d periodic leaky-wave antenna. *IEEE Transactions on Antennas and Propagation*, *67*(6), 3560–3573.
24. Nguyen, H. V., Abielmona, S., Rennings, A., Caloz, C. (2007). Pencil-beam full-space scanning 2D CRLH leaky-wave antenna array. In *2007 international symposium on signals, systems and electronics, Montreal, QC* (pp. 139–142).
25. Tianxia Zhao, D. R., Jackson, J. T., Williams, H. D. Y., & Oliner, A. A. (2005). 2-D periodic leaky-wave antennas-part I: Metal patch design. *IEEE Transactions on Antennas and Propagation*, *53*(11), 3505–3514.
26. Zhao, T., Jackson, D. R., & Williams, J. T. (2005). 2-D periodic leaky-wave Antennas-part II: Slot design. *IEEE Transactions on Antennas and Propagation*, *53*(11), 3515–3524.
27. Al-Shalaby, N. A., Elhenawy, A. S., Zainud-Deen, S. H., & Malhat, H. A. (2021). Electronic Beam-scanning strip-coded graphene leaky-wave antenna using single structure. *Plasmonics*, *16*(4), 1427–1438.

28. Podilchak, S. K., Freundorfer, A. P., & Antar, Y. M. M. (2008). Planar leaky-wave antenna designs offering conical-sector beam scanning and broadside radiation using surface-wave launchers. *IEEE Antennas and Wireless Propagation Letters*, 7, 155–158.
29. Anderson, T. (2011). *Plasma antennas*. Artech House.
30. De Carlo, P., Magarotto, M., Mansutti, G., Selmo, A., Capobianco, A.-D., & Pavarin, D. (2021). Feasibility study of a novel class of plasma antennas for satcom navigation systems. *Acta Astronautica*, 178, 846–853.
31. Zainud-Deen, S. H., & Malhat, H. A. (2019). Electronic beam switching of circularly polarized plasma magneto-electric dipole array with multiple beams. *Plasmonics*, 14(4), 881–890.
32. Podilchak, S. K., Freundorfer, A. P., Antar, Y. M. M. (2008) Novel planar antennas using circular, curved and straight gratings for conical-sector beam patterns. In *2008 38th European microwave conference* (pp. 539–542)
33. Zainud-Deen, S. H., Malhat, H. A., El-shalaby, N. A., & Gaber, S. M. (2019). Circular polarization bandwidth reconfigurable gain planar plasma helical antenna. *IEEE Transactions on Plasma Science*, 47, 4274–4280.
34. Malhat, H. A., Elhenawy, A. S., Zainud-Deen, S. H., & El-Shalaby, N. A. (2021). 1-D reconfigurable graphene strips leaky wave antenna with different feeders for wide scanning angles. *International Journal of RF and Microwave Computer-Aided Engineering*, 31(7), e22683.
35. Podilchak, S. K., Freundorfer, A. P., & Antar, Y. M. M. (2008). Broadside radiation from a planar 2-D leaky-wave antenna by practical surface-wave launching. *IEEE Antennas and Wireless Propagation Letters*, 7, 517–520.
36. Comite, D., et al. (2018). Radially periodic leaky-wave antenna for bessel beam generation over a wide-frequency range. *IEEE Transactions on Antennas and Propagation*, 66(6), 2828–2843.
37. Sarabandi, K., Jam, A., Vahidpour, M., & East, J. (2018). A novel frequency beam-steering antenna array for submillimeter-wave applications. *IEEE Transactions on Terahertz Science and Technology*, 8(6), 654–665.
38. You, Y., Lu, Y., You, Q., Wang, Y., Huang, J., & Lancaster, M. J. (2018). Millimeter-wave high-gain frequency-scanned antenna based on waveguide continuous transverse stubs. *IEEE Transactions on Antennas and Propagation*, 66(11), 6370–6375.
39. Attar, A., & Sebak, A. R. (2021). High gain periodic 2-D leaky-wave antenna with backward radiation for millimeter-wave band. *IEEE Open Journal of Antennas and Propagation*, 2, 49–61.
40. Al Shalaby, N., & El-Sherbiny, S. G. (2019). Mutual coupling reduction of DRA for MIMO applications. *Advanced Electromagnetics*, 8(1), 75–81.

Publisher's Note Springer Nature remains neutral with regard to jurisdictional claims in published maps and institutional affiliations.



Hend A. Malhat was born in Menouf, Egypt, on December 12, 1982. She received the B.Sc. and M.Sc. degrees from Menoufia University in 2004 and 2007, respectively. She received her Ph.D. degree in Antenna Engineering from Menoufia University, Egypt in 2011. She is currently an Associate Professor in the Department of Electrical and Electronic Engineering in the Faculty of Electronic Engineering, Menoufia University, Egypt. Her research interest at present includes graphene antennas, plasma antennas, wavelet techniques, transmitarray, reflectarray and RFID.



Abdelkarim S. Elhenawy was born in Saudi Arabia, on November 16, 1995. He received the B. Sc degree from Kafrelsheikh University in 2018. He is currently a demonstrator in the department of electrical engineering in the Faculty of Engineering, Kafrelsheikh University, He is currently working for M.Sc degree in Antenna Engineering from Menoufia University. His research interest at present include Plasma, Graphene, Leaky wave antennas, Reconfigurable antennas, and beam scanning.



Saber H. Zainud-Deen was born in Menouf, Egypt, on November 15, 1955. He received the B.Sc. and M.Sc. degrees from Menoufia University in 1973 and 1982, respectively, and the Ph.D. degree in Antenna Engineering from Menoufia University, Egypt in 1988. He is currently a Professor in the Department of Electrical and Electronic Engineering in the Faculty of Electronic Engineering, Menoufia University, Egypt. His research interest at present include microstrip and leaky wave antennas, DRA, RFID, optimization techniques, FDFD and FDTD, scattering problems and breast cancer detection.



Noha A. Al-Shalaby was born in El-Gharbya, Egypt, on November 15, 1975. She received the B.Sc. and M.Sc. degrees from Tanta University in 1998 and 2005 respectively. She received her Ph.D. degree in Antenna Engineering from Menoufia University, Egypt 2013. She is currently An Associate Professor in the department of electrical engineering in the Faculty of Engineering, Kafrelsheikh University, Egypt. Her research interest at present include plasma antennas, DRA, transmitarray, reflectarray and RFID.